Tellus (1986), *38A*, 49–59

The kinetic and available potential energy budget of a winter extratropical cyclone system

By PHILLIP J. SMITH and PATRICIA M. DARE, *Department of Geosciences, Purdue University, West Lafayette, IN 47907, USA*

(Manuscript received December 11, 1984; in final form April 17, 1985)

ABSTRACT

The energy budget of an extratropical cyclone system which traversed North America and intensified through the period 9–11 January 1975 is presented. The objectives of the study are (1) to document the complete energy budget of a significant winter cyclone event, and (2) to comment on the significance of latent heat release (LHR) in the cyclone's evolution. Results reveal an overall increase in both kinetic (K) and available potential energy (A). K increases are accounted for by boundary flux convergence of K, while A increases are due to generation by LHR and K to A conversion. In addition, the general A increase is accompanied by a 24 h oscillation that is explained largely by the flux quantity in the A budget equation and is correlated with a similar fluctuation in the K to A conversion.

LHR does not appear to be critical in the development of this cyclone system. Rather, LHR acts to increase the intensity of the event. It is hypothesized that the direct influence that LHR had on the deepening cyclone's reduced mass was augmented by an indirect influence, in which pre-existing dry dynamical forcing was enhanced by diabatic heating, thus leading to accelerated cyclone development at a later time.

1. Introduction

Over the past 15 to 20 years, a useful technique for diagnosing the observed behavior of extratropical cyclones has been to evaluate their energy budgets. Most of these investigations have been case studies of individual cyclone events (see, for example, the review by Smith (1980)), although a notable effort to establish the mean energetics of cyclones was published by Kung and Baker (1975). The bulk of published works in this field have dealt only with particular components of the energy budget. The most commonly described components have been those contained in the kinetic energy budget, while the diabatic generation of available potential energy has been a subject of special interest in a number of other papers. Few have presented diagnoses of the complete energy budget of cyclone systems. Such a diagnosis is presented in this paper.

The present diagnosis focuses on an intense, winter cyclone associated with a strong, well-developed jet stream and abundant precipitation and latent heat release. This case has been previously studied by our group with the primary objective being to establish the role of latent heat release in the evolution of the cyclone. The methodology has included both numerical model experimentation (Robertson and Smith, 1983; Kenney and Smith, 1983) and observational data analyses (Dare and Smith, 1984; Smith, et al., 1984). This paper represents an extension of the latter of these studies and has as its principle objectives:

(1) to document the complete energy budget of a significant winter cyclone event;

(2) to further comment on the significance of moist processes in the cyclone's evolution.

2. Budget equations

The energetics of the observed large-scale motion fields in a hydrostatic atmosphere can be examined through the Eulerian kinetic energy budget equation, given by Smith (1980) as

$$\frac{\partial K}{\partial t} = \int - \mathbf{V}\cdot\nabla\phi + \int - \nabla\cdot k\mathbf{V} - \int \frac{\partial \omega k}{\partial p} + \int \mathbf{V}\cdot\mathbf{F}, \quad (1)$$

where

$\int = (1/g\sigma) \iiint \mathrm{d}x\,\mathrm{d}y\,\mathrm{d}p$;

K = kinetic energy content, $\int k$;

k = horizontal kinetic energy per unit mass, $\frac{1}{2}(u^2 + v^2)$;

V = horizontal wind vector with components (u, v);

σ = area of the computational region;

$g = 9.80$ m s^{-2};

$\phi = gz$;

z = geopotential height of pressure surfaces;

p = pressure;

ω = vertical motion in isobaric coordinates, $\mathrm{d}p/\mathrm{d}t$;

∇ = horizontal del operator on a pressure surface;

x, y = west–east, south–north coordinates in a spherical curvilinear coordinate system.

Left to right the terms in (1) represent the local rate of change (DK), mechanical generation by cross-contour flow (GK), horizontal and vertical flux divergence (BFK), and dissipation (DIS) of kinetic energy.

The corresponding Eulerian available potential energy budget equation is from Smith, et al. (1977),

$$\frac{\partial A}{\partial t} = \int E\dot{Q} + \int \omega\alpha + \int - \nabla\cdot c_p \mathrm{ET}V + \int - \frac{\partial}{\partial p} c_p \mathrm{ET}\omega + \int - \frac{c_p T}{p^\kappa}\frac{\mathrm{d}p_r^\kappa}{\mathrm{d}t}, \quad (2)$$

where

A = available potential energy content, $\int c_p$ ET;

E = efficiency factor (Dutton and Johnson, 1967), defined for the computational region as $(p^\kappa - p_r^\kappa)/p^\kappa$;

p_r = reference pressure, defined at each point as the area average (over the computational region) pressure on the potential temperature surface passing through that point;

$\dot{Q}$ = diabatic heating rate per unit mass;

T = temperature

α = specific volume;

$\kappa = R/c_p = 0.286$.

Left to right, the terms in (2) are the local rate of change (DA), diabatic generation (GA), release (CA), and horizontal and vertical flux divergence (BFA) of A. The last term (DP) is the local change of A caused by the integrated change of the reference pressure. Eqs. (1) and (2) can be coupled by noting that

$$\mathrm{CA} = -\mathrm{GK} + \int - \nabla\cdot\phi V + \int - \frac{\partial \omega\phi}{\partial p}, \quad (3)$$

where the last two right-hand-side terms are often referred to as the boundary work terms (BW).

Although (2) describes the fundamental processes influencing A, use of this equation does pose two problems. First, comparison of (1) and (2) reveals that no direct A to K conversion process is explicitly identified. Second, despite its use by Lin and Smith (1982) and Robertson and Smith (1983), DP has not yet been given a completely satisfactory physical description. A remedy to both problems has been recently proposed by Robertson (1985). In this he replaces CA in (2) by −GK + BW from (3) and further shows that

$$\mathrm{DP} = \int \nabla\cdot\phi_r V + \int \frac{\partial \omega\phi_r}{\partial p}, \quad (4)$$

where ϕ_r is the reference state value for ϕ and the right-hand-side terms become the negative of reference state boundary work (−BWR). Thus, inserting (3) and (4) in (2) yields

$$\mathrm{DA} = \mathrm{GA} - \mathrm{GK} + \mathrm{BFA} + \mathrm{BW} - \mathrm{BWR}. \quad (5)$$

Further simplification is possible by combining the last three terms, all of which involve boundary fluxes. Note that the fluxed quantities are, from (2), (3) and (4), c_p ET + $\phi - \phi_r$. Since $c_p T + \phi$ is the dry static energy, c_p ET + $\phi - \phi_r$ can be described as the available dry static energy. Thus, (5) becomes

$$\mathrm{DA} = \mathrm{GA} - \mathrm{GK} + \mathrm{BFS}. \quad (6)$$

This last form of the available potential energy budget equation is applied in this study. Note that the baroclinic potential to kinetic energy conversion process is represented in (6) by GK, as suggested by Smith (1970). Finally, additional terms in (1), (2), (5), and (6) involving the Eulerian derivatives of the upper and lower pressure levels have been omitted because the upper pressure level is held fixed and the contribution from the lower level (surface) pressure change is small.

3. Data and computational methods

The original data for this case were mandatory-level rawinsonde observations from 99 North American stations taken at the standard 12 h interval from 1200 GMT 9 January to 1200 GMT 11 January 1975. Humidity data were supplemented by significant level data. Missing temperature and moisture data were supplied by vertical linear interpolation, while missing wind data were interpolated using the scheme described by Chien and Smith (1973). In addition, observational data were examined to isolate reports which were not representative of the synoptic scale. In such cases the data were replaced by bogused values derived from NMC analyses. Finally, data were bogused at three boundary points, located at 130° W and 30°, 40°, and 50° N, in order to augment the coverage over the data-sparse eastern Pacific Ocean. The station distribution is shown in Fig. 1.

The mandatory-level data were then interpolated to standard pressure levels extending upward to 100 mb in 50 mb increments, with heights determined from the hypsometric equation. Interpolated winds were also vertically filtered using a three-point binomial smoother (Ward and Smith, 1976). Finally, in order to provide "data" needed in the objective analysis and the finite difference calculations, observational data were extrapolated below ground to standard pressure levels extending to 1050 mb. These 1050 to 100 mb data were then analyzed to a 1.25° latitude by 1.603° longitude grid extending from 70° to 134° W and 17.5° to 60° N (41 x 35 point grid, see dashed boundary in Fig. 1) using the Barnes objective analysis scheme (Barnes, 1973; Maddox, 1980). The characteristics of the analysis are determined by parameters C and G, which were chosen to yield a response of 0.46 at the minimum resolvable wavelength of the rawinsonde network, cited by Maddox as 800 km. The values of C and G used were 40,000 and 0.35, respectively, following Maddox's example. The vertical motion fields were obtained by applying the adjusted kinematic method (O'Brien, 1970; Chien and Smith, 1973) to the gridded wind data with zero boundary conditions at the surface and 100 mb.

The energetics calculations were carried out on a 29 x 20 point domain roughly the size of the contiguous United States (75–120° W, 30–

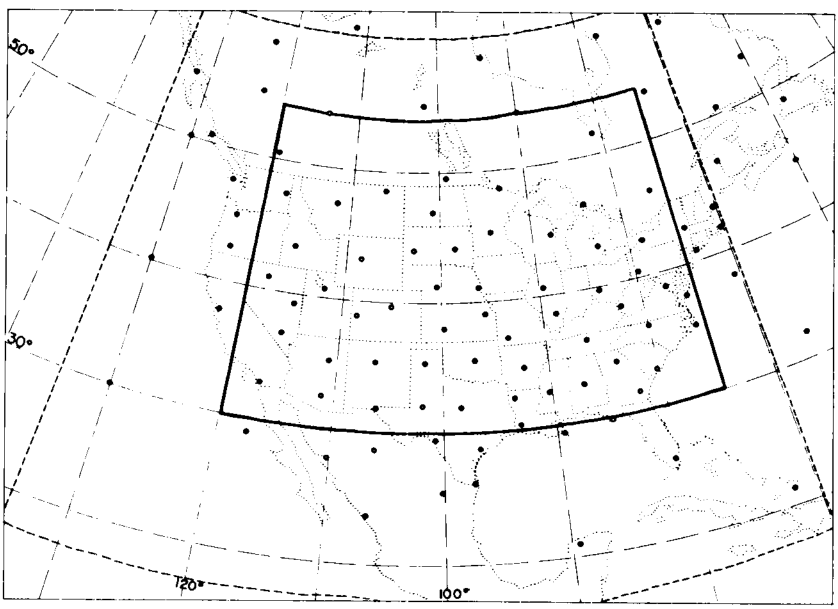

Fig. 1. Rawinsonde station distribution (circles), analysis domain (dashed boundary), and computational domain (solid boundary).

53.75° N; see Fig. 1). The calculations were performed from 1050 to 150 mb. However, vertical integrations were carried out from the surface upwards, so that the mass of the fictitious atmosphere below the surface was not added to the atmosphere. Second-order horizontal and vertical differencing was used throughout, except at the lower boundary, where first-order vertical differencing was used. Tendencies of the energy contents (DK and DA) were calculated as 12 h differences, while DIS and BFS were calculated as residuals required to balance their respective equations. Error characteristics of the various budget calculations have been described by Vincent and Chang (1975), Kornegay and Vincent (1976), Ward and Smith (1976), Vincent et al. (1977b), Chen and Bosart (1977), Robertson and Smith (1980), Lin and Smith (1982), and Dare and Smith (1984).

The diabatic heating contributions represented in GA were restricted to the latent heat release. Results of Vincent et al. (1977a) and Lin and Smith (1982) indicate that this contribution comprises the bulk of GA for a moist extratropical cyclone. The latent heating values were calculated as the sum of separately calculated convective and stable components.

The convective component was determined using Kuo's (1965, 1974) parameterization scheme with the modifications described by Edmon and Vincent (1976) and Lin and Smith (1979). In the Kuo scheme, the convective latent heat release (CLHR) is parameterized by

$$\mathrm{CLHR} = \frac{g(1-b)\,LM_t[T_c(p)-T(p)]\,\theta/T}{(p_b-p_t)\langle T_c-T\rangle}, \qquad (7)$$

where

M_t = rate of moisture convergence from the surface to the cloud top, including horizontal convergence of specific humidity and evaporation of water from the lower surface;

T_c = temperature within the cloud, assumed to be the temperature of the moist adiabat extending from the cloud base;

θ = potential temperature;

L = latent heat of condensation,
$= 2.501 \times 10^6$ J kg^{-1} for $T \geqslant -20$ °C,
$= 2.835 \times 10^6$ J kg^{-1} for $T < -20$ °C;

p_b = pressure at the cloud base, the base of the first conditionally unstable layer;

p_t = pressure at the cloud top, the level at which the moist adiabat from the cloud base crosses the environmental sounding;

$$\langle T_c - T\rangle = \frac{1}{p_b-p_t}\int_{p_t}^{p_b}(T_c-T)\,\mathrm{d}p;$$

b = the fraction of M_t stored in the air to increase the specific humidity of the environment.

This latter quantity is typically assumed to be zero, in response to Kuo's (1974) suggestion that b is much smaller than one in regions of low-level convergence in tropical regions. However, in an extratropical region, b may not always be near zero. To allow for this possibility, the mean relative humidity from the surface to 500 mb (RHAV) was used as the background relative humidity in the following procedure. If the value of RHAV $\leqslant 0.4$, b was assumed to be unity. In the Kuo scheme this means that all converged moisture is stored and no convective latent heat release occurs. This is consistent with the mean relative humidity constraint introduced for this scheme by Lin and Smith (1979) and compares with the critical value of 0.5 used by Anthes (1977b) for a hurricane case. If RHAV $\geqslant 0.8$, b was assumed to be zero. The upper bound value for RHAV was chosen to correspond with the relative humidity constraint imposed on the stable precipitation. If RHAV was between these two limiting values, then b = 1-RHAV, a form similar to that proposed by Anthes (1977a).

The stable component was calculated in the same fashion as Krishnamurti and Moxim (1971) and Vincent, et al. (1977a), in which the stable latent heat release is proportional to the vertical advection of saturation specific humidity. Stable latent heat release is allowed under the following conditions: (1) upward vertical motion, (2) vertical moisture convergence for saturated air at environmental temperatures, and (3) relative humidity $\geqslant$80%. Both heating components were allowed to occur simultaneously.

4. Synoptic case

The 9–11 January 1975 cyclone event, depicted in Fig. 2, is an example of strong baroclinic development which was initially dry and then was

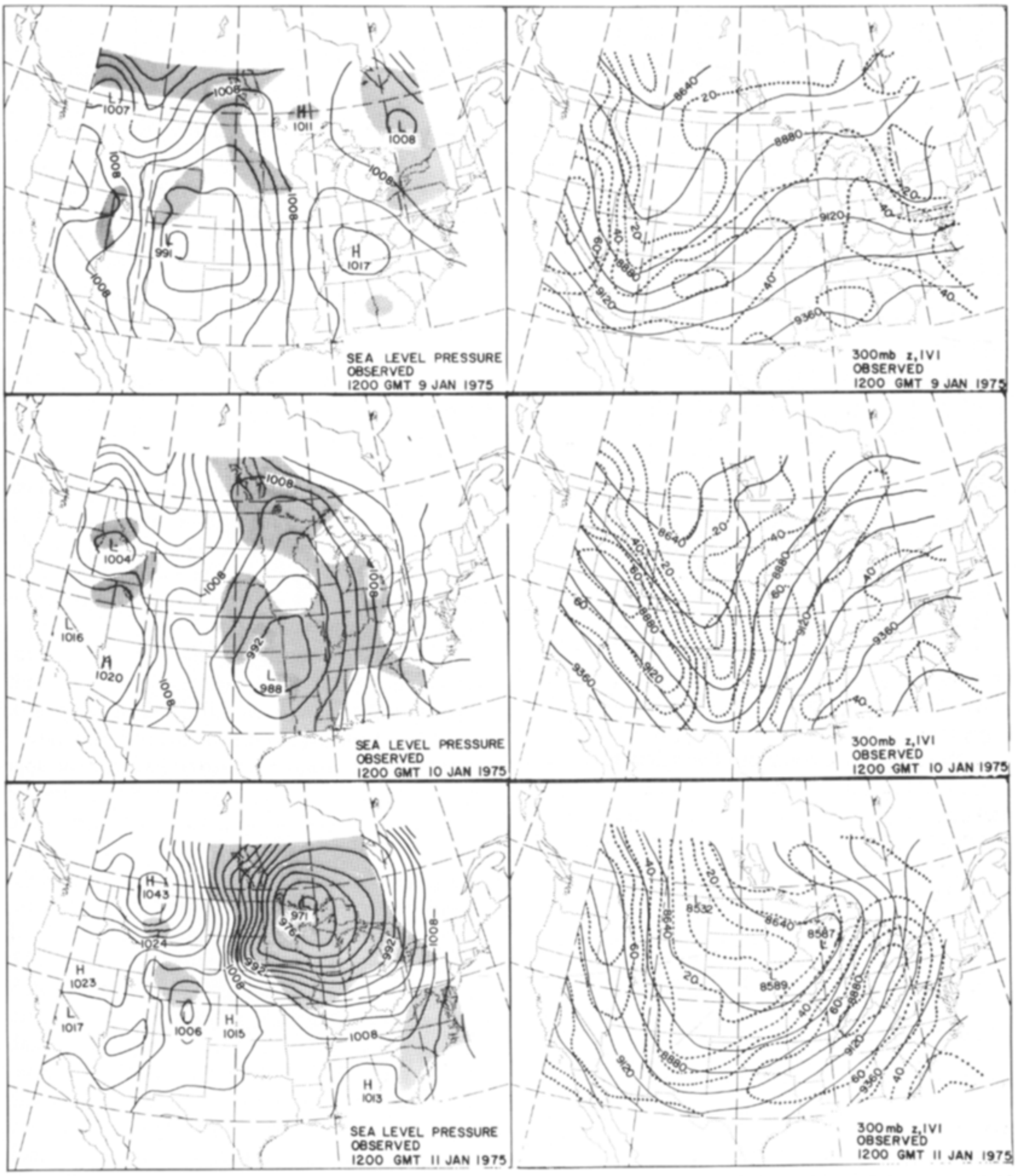

Fig. 2. Sea level pressure (mb) and 300 mb heights (m, solid) and isotachs (m s^{-1}, dashed) for 1200 GMT 9–11 January 1975. Shaded areas encompass stations reporting precipitation at each map time.

accompanied by abundant latent heat release. At the initial time (1200 GMT 9 January) a large cyclone was centered over southern Colorado with a supporting upper-air trough lying along the Rocky Mountains. After an initial 12 h period during which the surface low exhibited little change, rapid development took place, accompanied by prefrontal convection and widespread stable precipitation. By 1200 GMT 10 and 11 January, the central sea level pressure had decreased from an initial value of 991 mb to 988 and 971 mb, respectively. This deepening was accompanied by intensification of the upper-air wave and development of a closed circulation at 500 mb. A more detailed synoptic discussion of this case is presented in Kenney and Smith (1983) and Dare and Smith (1984).

5. Total energy budget

The available potential and kinetic energy budgets for the cyclone system are summarized in Table 1. Considering first the *A* budget, one immediately sees a general increasing trend in *A* with a strong superimposed 24 h oscillation. Maxima in *A* occur at 1200 GMT and minima at 0000 GMT. Paralleling this oscillation is a similar 24 h fluctuation in −GK. Conversions from *A* to *K* (negative values of −GK) are generally indicated at 1200 GMT and from K to A at 0000 GMT. While the correlation between *A* and −GK may be

Table 1. *Area-averaged, vertically integrated energy budgets (A and K, 10^5 J m^{-2}; other quantities W m^{-2}) and cyclone central sea level pressure (p_s, mb)*

Date/time (GMT)	*A*	DA	GA	−GK	BFS	p_s
9/1200	28.8		−0.1	−6.1		991
		−18.1			−32.6	
10/0000	21.0		0.7	34.5		991
		43.1			18.8	
10/1200	39.6		15.9	−2.5		988
		−36.1			−53.0	
11/0000	24.0		8.8	11.6		980
		30.1			17.0	
11/1200	37.2		5.5	0.4		971
Date/time (GMT)	***K***	**DK**	**BFK**	**GK**	**DIS**	**p_s**
9/1200	30.3		19.3	6.1		991
		9.5			−5.4	
10/0000	34.4		39.0	−34.5		991
		10.4			−10.1	
10/1200	38.9		34.0	2.5		988
		11.8			−20.6	
11/0000	44.0		39.9	−11.6		980
		16.7			−17.2	
11/1200	51.2		39.8	−0.4		971

fortuitous, these integrated values suggest that conversions from *A* to *K* are more pronounced within the system when *A* is larger, i.e., when the baroclinicity within the system is greatest.

The corresponding oscillation in the *A* tendency (DA) is similar to that found in BFS, indicating that changes in available potential energy are strongly influenced by flux convergence or divergence of existing and reference state temperature and geopotential. In addition, note that the generation of *A* by latent heat release (GA) does not assume a prominent role until the central map time (1200 GMT 10 January). This is accompanied by rapid lowering of the central pressure, decreased tendency to convert kinetic to potential energy, and increased kinetic energy changes. All of the latter are indicative of an intensifying system.

The *K* budget shows monotonically increasing *K* values. While GK exhibits the oscillations previously noted, the primary source and sink quantities (BFK and DIS, respectively) are quite stable. Both BFK and DIS are responding to the strong and persistent jet stream flow present in the region (see Fig. 2). At the same time, as described by Dare and Smith (1984) and previously reported by Ward and Smith (1976), the strong flux convergence is accompanied by abundant supergradient flow and negative GK values. This latter feature and the relationship to *A* previously noted indicate that the potential/kinetic energy conversion is on the whole responsive to the flux convergence of *K*; however, strong flux convergence is less likely to force kinetic to potential energy conversions (GK < O) when the baroclinicity of the system is stronger (larger *A*).

Further insight into the relationships between *A*, *K*, GK, BFK can be achieved by examining the time/pressure cross sections depicted in Fig. 3. In this presentation, BFK is represented by its horizontal flux component, identified as HFK. The available potential energy cross-section reveals that the 24 h oscillation noted in the Table 1 statistics is largely confined to the mid-troposphere, centred in the 650–600 mb layer. However, the corresponding oscillation in GK is centred in the upper troposphere, where *K* is maximum and where similar fluctuations in HFK are found. Thus, the conversion of potential to kinetic energy is dominant at jet stream levels and oscillates in the same fashion as horizontally fluxed kinetic energy at the same level and baroclinicity some 300 to 400 mb below. In the lower troposphere the energy

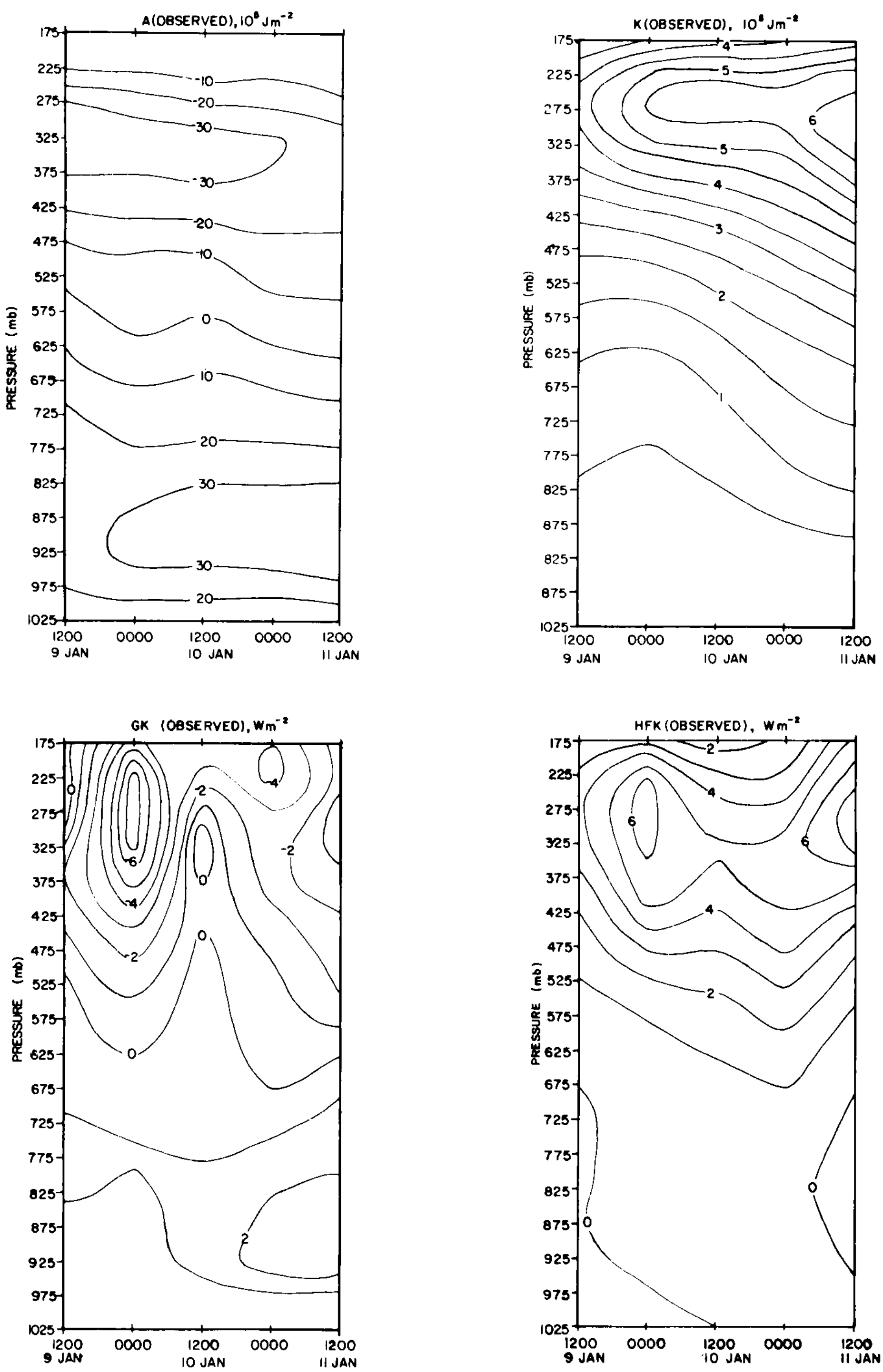

Fig. 3. Time/pressure cross-sections of area averaged A, K, GK, and HFK. Units: A and K, 10^5 J m^{-2}; GK and HFK, W m^{-2}.

quantities exhibit a much more regular behavior. As the cyclone intensifies, the energy levels and transformations monotonically increase.

A final summary of the total energy budget is presented in Fig. 4. Also included for comparison are results for the April 3–5 1974 cyclone reported by Robertson and Smith (1980) and Lin and Smith (1982). The GA value for the latter case includes only Lin and Smith's latent heat release contribution, in order to be comparable to the present study. For the January case, the figure summarizes the overall increase in both available potential and kinetic energy. In addition, it shows that the overall energy source for A is the conversion of K to A and generation of A by latent heat release and for K is the flux convergence of K, while the overall sink for A is the flux divergence of S and for K is the K to A conversion and dissipation of K.

Comparison with the April case reveals both striking similarities and differences. Fundamentally, the April case is similar in that it also represents a case of overall increasing energy levels, although smaller than the January case. The smaller April values reflect a weaker cyclone event (minimum central pressure 980 mb versus 971 mb for the January case) and earlier occlusion. The weaker April event is also indicated by the smaller A, K, and flux values. However, despite the fact that it is weaker, the April cyclone exhibits very similar generation of A and dissipation of K. These suggest a similar rôle for latent heat release and the presence of strong wind shears in both cases. The most striking difference is in the A to K conversion, which is similar in magnitude for the two cases but opposite in sign. This sign reversal appears to be a response to the order of magnitude difference in the flux divergence of K, as previously noted and referenced to Ward and Smith (1976) and Dare and Smith (1984).

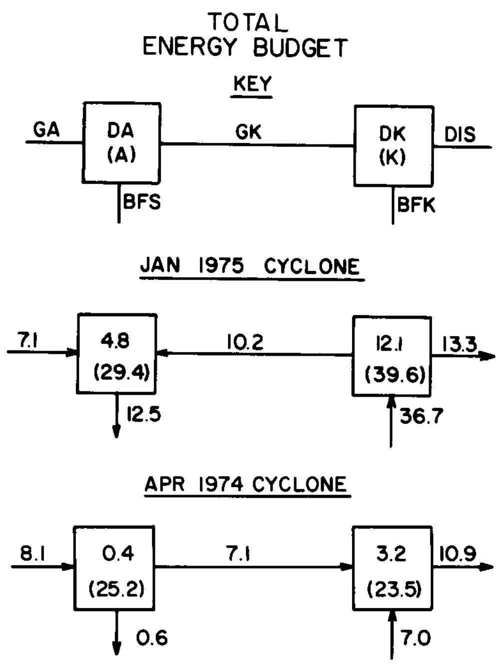

Fig. 4. Block diagrams representing time mean energy budgets for the present case and an April 1974 case (Robertson and Smith, 1980; Lin and Smith, 1982). Units: A and K, 10^5 J m^{-2}; other quantities, W m^{-2}.

6. Significance of moist processes

The precipitation fields associated with the developing cyclone are outlined in Fig. 2. The evolution of the fields is more fully discussed in Smith et al. (1984). For the present discussion it is sufficient to refer to Fig. 2 and Table 2, which summarizes the average total latent heat release calculated using the procedures identified in Section 3. Table 2 reveals that the evolution of moist processes in the cyclone system can be characterized in phases. The first 12 h is a dry phase, with only light precipitation; the second 12 h is a transition phase from dry to moist conditions as the cyclone's precipitation field increases in intensity and areal coverage. The third and fourth 12 h periods are, respectively, a moist phase encompassing fully-developed convective and stable

Table 2. *Vertically-integrated total (convective plus stable) latent heat release (TLHR) averaged over the computational domain*

Time (GMT)/date	TLHR (mm h^{-1})
1200/9 January	0.06
0000/10 January	0.15
1200/10 January	0.57
0000/11 January	0.25
1200/11 January	0.09

precipitation and another transition phase as the domain returns to a drier condition in the wake of the cyclone. Considering these phases, we have elected to focus attention on the first (dry phase) and third (moist phase) periods in order to highlight the role of moist processes.

The energy budget diagrams for these two periods are presented in Fig. 5. First note that the signs of the different energy transformations are the same for both periods. Furthermore, except for the dry phase diabatic generation of A, none of the quantities are negligible. These observations suggest that the cyclone is strongly influenced by a background set of dry dynamical forcing processes that are present early in the cyclone's development and persist as the cyclone intensifies. This suggestion is supported by Robertson and Smith's (1983) comparison of moist and dry numerical predictions of this case. They found that even in the absence of latent heat release (dry model prediction) a significant cyclone was predicted, although the dry cyclone was weaker than that obtained in the moist prediction.

These results further indicate that one of the rôles played by latent heat release is to alter the pre-existing dry dynamical forcing processes. The increased available potential and kinetic energy values suggest that both the temperature and geopotential height gradients have been enhanced in the moist phase, enhancements which are accompanied by much stronger flux divergence of available static energy and significantly reduced conversion of kinetic to potential energy (GK). In addition, the corresponding stronger flow is accompanied by increased flux convergence of K (BFK) and much greater dissipation of K. It is particularly interesting to note that the overall presence of supergradient flow (GK < 0) is less during the moist phase even though BFK is greater.

A further view of the importance of moist processes is seen in Fig. 6. Depicted here are graphs of two energy parameters that respond directly to latent heat release, generation of available potential energy (GA) and release of potential energy (CA, see eq. (2)), and two that

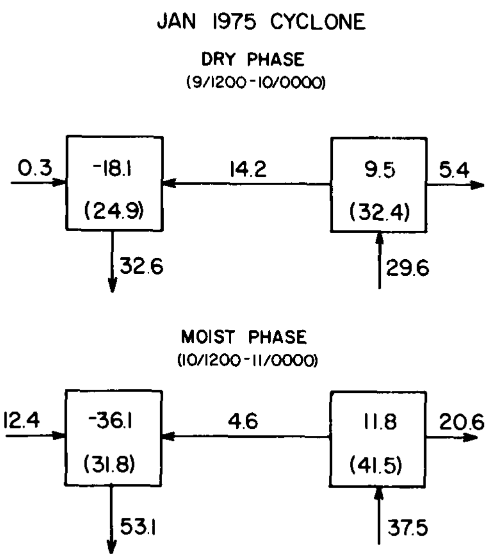

Fig. 5. Dry phase (1200 GMT 9 January–0000 GMT 10 January) and moist phase (1200 GMT 10 January–0000 GMT 11 January) energy budget diagrams. Diagram key and units as in Fig. 4.

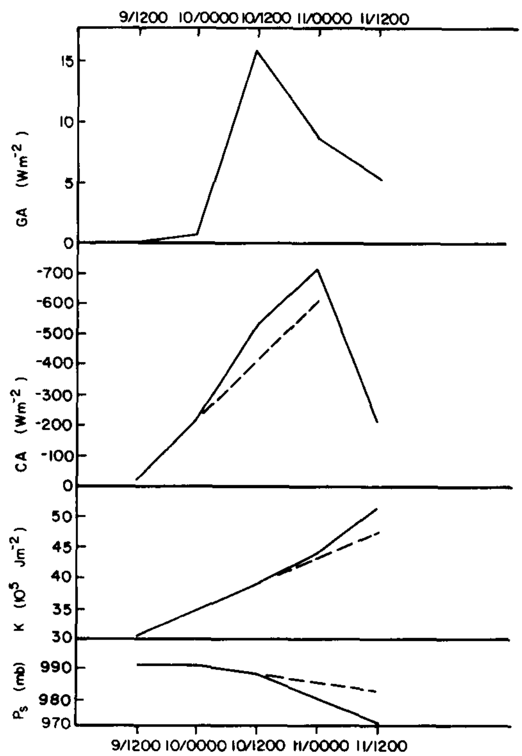

Fig. 6. Time profile of vertically-integrated, area-averaged GA, CA, K and p_s. Solid lines represent calculated values; dashed lines represent dry simulated values (see text for explanation). Units: K, 10^5 J m^{-2}; GA and CA, W m^{-2}; p_s, mb.

represent measures of the intensity of the cyclone system, kinetic energy content (K) and central sea level pressure (p_s). As expected, GA is very small during the dry phase, peaks at 1200 GMT 10 January and then diminishes. The distinction between the dry and moist phases is quite clear for this parameter. In contrast the release of potential energy increases in intensity steadily through 0000 GMT 11 January, 12 h after the maximum GA and maximum latent heat release. The decrease at the last map time likely is because an influential part of the upward motion region has moved outside of the computational domain. In a similar way the kinetic energy increases and the central pressure decreases throughout the period. In fact, the rate of these changes is greater after the maximum latent heat release time. All of this suggests that not only does latent heat release enhance the development of the cyclone, but also that at least a portion of this enhancement results from an indirect role played by the heating field, namely the enhancement of dry dynamical forcing which in turn leads to additional cyclone development at a later time.

Finally, Fig. 6 contains "simulation" curves intended to hypothesize the course of events had latent heat release not occurred. The dashed line that represents this simulation is constructed by extending the trend established during the dry phase of the cyclone's development. The p_s curve is extended from the transition phase trend because no p_s change occurred during the dry phase. The differences between the solid and dashed lines are intended to convey a general impression of the enhancement attributable to latent heat release. Comparison of the lines suggest a central pressure difference of about 12 mb and energy level differences of 10 to 15% at the final map time. These results are similar to those of Dare and Smith (1984), in which the moist and dry predictions of this event at 1200 GMT 11 January differed by 6 mb in the central pressure and 13.5% in the eddy kinetic energy content. Thus, even in the absence of latent heat release the dry dynamical forcing would have been sufficient in this case to produce a significant cyclone event.

7. Summary

This paper described the energy budget of a cyclone system characterized by decreasing pressure, increasing kinetic energy, and increasing available potential energy. The primary source for the K increases is the boundary flux convergence, while for the A increases it is the combined influence of generation by latent heat release and conversion of K to A. While the trend in K is monotonic throughout the cyclone system's evolution, the overall upward trend in A is modulated by a 24 h oscillation. This oscillation is primarily influenced by a similar fluctuation in the boundary flux of available static energy and, in addition, is well-correlated with temporal changes observed in A/K conversion. In the latter, conversion from A to K is more pronounced when A is larger, i.e., when the baroclinicity of the system is greater.

It appears that this case represents an example of an intense extratropical cyclone that is a member of a more general class of cyclones that are responsive to, but not dependent on attending latent heat release. While the intensity of the cycline no doubt depends of latent heat influence, it seems likely that a significant event could have developed even in the absence of moist processes. Finally, we hypothesize that the rôle of latent heat release may be two-fold. First, the released heat could "directly" reduce the cyclone's mass field. Second, the heating could enhance the pre-existing dry dynamical forcing and thus "indirectly" lead to accelerated cyclone development at a later time.

All of this suggests fruitful avenues of future research. For example, the validity of the direct/indirect influence needs to be more thoroughly explored by examining the temporal and spatial evolution of the dry dynamical forcing in both the presence and absence of latent heat release. Such a study is now in progress using numerical model simulations. In addition, it would be of interest to study the class of cyclones that are in fact quite dependent on the presence of latent heat release. Such a case was included in Robertson and Smith (1983). However, it remains to explore the form that this dependence takes.

8. Acknowledgments

The authors are indebted to Helen Henry for typing the manuscript, to Kenneth Wilson and Daniel Vietor for data tabulations and figure drafting, and to the referees for their thoughtful suggestions. A portion of this research was completed while the second author was a National Science Foundation Fellow, during which computing support was provided by the Purdue University Computing Center. In addition, a significant portion of the work was supported by NASA contract NAS 843009.

REFERENCES

Anthes, R. A. 1977a. A cumulus parameterization scheme utilizing a one-dimensional cloud model. *Mon. Wea. Rev. 105*, 270–286.

Anthes, R. A. 1977b. Hurricane model experiments with a new cumulus parameterization scheme. *Mon. Wea. Rev. 105*, 287–300.

Barnes, S. L. 1973. Mesoscale objective map analysis using weighted time series observations. NOAA Tech. Memo. ERL NSSL-62, 60 pp. (NTIS COM 73-10781).

Chen, T. and Bosart, L. F. 1977. Quasi-Lagrangian kinetic energy budgets of composite cyclone-anticyclone couplets. *J. Atmos. Sci. 34*, 452–464.

Chien, H. and Smith, P. J. 1973. On the estimation of kinematic parameters in the atmosphere from radiosonde wind data. *Mon. Wea. Rev. 101*, 252–261.

Dare, P. M. and Smith, P. J. 1984. A comparison of observed and model energy balance for an extratropical cyclone system. *Mon. Wea. Rev. 112*, 1289–1308.

Dutton, J. A. and Johnson, D. R. 1967. The theory of available potential energy and a variational approach to atmospheric energetics. *Adv. Geophys. 12*, 333–436.

Edmon, H. J., Jr. and Vincent, D. G. 1976. An application of two tropical parameterization schemes of convective latent heat release in middle latitudes. *Mon. Wea. Rev. 104*, 1141–1153.

Kenney, S. E. and Smith, P. J. 1983. On the release of eddy available potential energy in an extratropical cyclone system. *Mon. Wea. Rev. 111*, 745–755.

Kornegay, F. C. and Vincent, D. G. 1976. Kinetic energy budget analysis during interaction of Tropical Storm Candy (1968) with an extratropical frontal system. *Mon. Wea. Rev. 104*, 849–859.

Krishnamurti, T. N. and Moxim, W. J. 1971. On parameterization of convective and non-convective latent heat release. *J. Appl. Meteorol. 10*, 3–13.

Kung, E. C. and Baker, W. E. 1975. Energy transformations in the middle-latitude disturbances. *Q. J. R. Meteorol. Soc. 101*, 793–815.

Kuo, H. L. 1965. On formation and intensification of tropical cyclones through latent heat release by cumulus convection. *J. Atmos. Sci. 22*, 40–63.

Kuo, H. L. 1974. Further studies of the parameterization of the influences of cumulus convection on large-scale flow. *J. Atmos. Sci. 31*, 1232–1240.

Lin, S. C. and Smith, P. J. 1979. Diabatic heating and generation of available potential energy in a tornado producing extratropical cyclone. *Mon. Wea. Rev. 107*, 1169–1183.

Lin, S. C. and Smith, P. J. 1982. The available potential energy budget of a severe storm-producing extratropical cyclone. *Mon. Wea. Rev. 110*, 521–533.

Maddox, R. A. 1980. An objective technique for separating macroscale and mesoscale features in meteorological data. *Mon. Wea. Rev. 108*, 1108–1121.

O'Brien, J. J. 1970. Alternative solutions to the classical vertical velocity problem. *J. Appl. Meteorol. 9*, 197–203.

Robertson, F. R. 1985. Reference pressure changes and available potential energy in isobaric coordinates. *Tellus 37A*, 24–29.

Robertson, F. R. and Smith, P. J. 1980. The kinetic energy budgets of two severe storm producing extratropical cyclones. *Mon. Wea. Rev. 108*, 127–143.

Robertson, F. R. and Smith P. J. 1983. The impact of model moist processes on the energetics of extratropical cyclones. *Mon. Wea. Rev. 111*, 723–744.

Smith, P. J. 1970. A note on energy conversions in open atmospheric systems. *J. Atmos. Sci. 27*, 518–521.

Smith, P. J. 1980. The energetics of extratropical cyclones. *Rev. Geophys. Space Phys. 18*, 378–386.

Smith, P. J., Dare, P. M. and Lin, S.-J. 1984. The impact of latent heat release on synoptic-scale vertical motions and the development of an extratropical cyclone system. *Mon. Wea. Rev. 112*, 2421–2430.

Smith, P. J., Vincent, D. G. and Edmon, H. J., Jr. 1977. The time dependence of reference pressure in limited region available potential energy budget equations. *Tellus 29*, 476–480.

Vincent, D. G. and Chang, L. N. 1975. Kinetic energy budgets of moving systems: Case studies for an extratropical cyclone and Hurricane Celia, 1970. *Tellus 27*, 215–233.

Vincent, D. G., Pant, G. B. and Edmon, H. J., Jr. 1977a. Generation of available potential energy of an extratropical cyclone system. *Mon. Wea. Rev. 105*, 1252–1265.

Vincent, D. G., Schlatter, T. W., Kornegay, F. C. and Edmon, H. J., Jr. 1977b. Comparison between the NACR multivariate statistical objective analysis scheme and subjective analysis in a limited region. *Beit. Phys. Atmos. 50*, 272–283.

Ward, J. H. and Smith, P. J. 1976. A kinetic energy budget over North America during a period of short synoptic wave development. *Mon. Wea. Rev. 104*, 836–848.